IEEE Photonics Journal
An IEEE Photonics Society Publication

Open Access

Maximum Entropy Method-Based Acceptor Triplet-State Fluorescence Correlation Spectroscopy Analysis for Determination of Donor–Acceptor Distance Distribution: Theory and Simulation

Volume 7, Number 3, June 2015

B. L. Chen
Z. Y. Guo
T. S. Chen

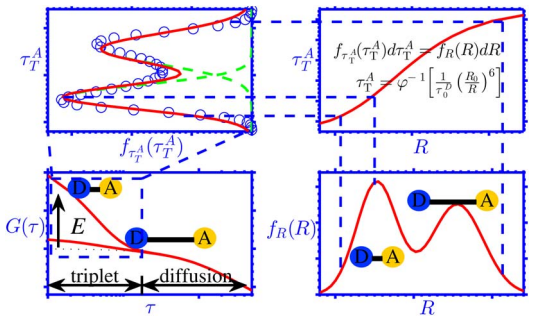

DOI: 10.1109/JPHOT.2015.2417168
1943-0655

Maximum Entropy Method-Based Acceptor Triplet-State Fluorescence Correlation Spectroscopy Analysis for Determination of Donor–Acceptor Distance Distribution: Theory and Simulation

B. L. Chen, Z. Y. Guo, and T. S. Chen

MOE Key Laboratory of Laser Life Science, Laboratory of Photonic Chinese Medicine, College of Biophotonics, South China Normal University, Guangzhou 510631, China

DOI: 10.1109/JPHOT.2015.2417168

Manuscript received March 3, 2015; accepted March 23, 2015. Date of publication March 26, 2015; date of current version June 3, 2015. This work was supported in part by the National Natural Science Foundation of China under Grant 81471699 and Grant 61178078 and in part by the Guangzhou Science and Technology Plan Project under Grant 2014J4100055. Corresponding author: T. S. Chen (e-mail: chentsh@scnu.edu.cn).

Abstract: A maximum entropy method-based acceptor triplet-state fluorescence correlation spectroscopy (tsFCS) analysis, i.e., tsFCS fluorescence resonance energy transfer (tsFCS-FRET), was proposed to resolve the donor–acceptor distance (R) distribution of a FRET system with multiple distances. An R-dependent acceptor triplet-state weight distribution function was introduced into the excited tsFCS model with a fixed R, and the weight distribution maximized the value of the Shannon entropy. tsFCS-FRET analysis showed consistent distributions with the actual pre-input for both unimodal distribution and two-species systems and a distribution with three peaks close to the pre-inputted values for three-species system at higher donor laser power. Collectively, tsFCS-FRET provides a powerful tool for resolving the R distribution, in turn, to the FRET efficiency (E) distribution, of a FRET system containing multiple E species.

Index Terms: Fluorescence resonance energy transfer (FRET), FRET efficiency (E), auto-correlation (AC), MemExp.

1. Introduction

Fluorescence resonance energy transfer (FRET) is an intermolecular photophysical process in which the donor (D) in the excited state transfers its energy to a nearby acceptor (A) by dipole-dipole coupling [1]. FRET occurs between molecules in close proximity at nanometer level (1–10 nm) and is known as "molecular ruler" because the energy transfer efficiency (E) is sixth power inversely proportional to the intermolecular separation (R) [2]. Recently, a strategy for measuring the FRET efficiency (E) based on triplet-state fluorescence correlation spectroscopy (tsFCS) analysis has been established [3]. In contrast to intensity-based fluorescence measurements [4], [5], FCS bases on fluctuation analysis for minute deviations from thermal equilibrium of small molecular ensembles, combining maximum sensitivity with high statistical confidence [6].

Triplet state (T) excitations are always along with fluorescence emissions in FCS measurements. Considerable population of the triplet state is generated, even though the fluorophore is

irradiated with a moderate excitation power [7]. The fluctuation caused by the transition of excited singlet-triplet state gives rise to a fast correlation time region in the auto-correlation (AC) curve. An electronic three states model were proposed to quantitatively estimate the influence of triplet state excitations on AC curve [8]. By solving a thermodynamic equilibrium system of three first-order differential equations according to this model, the population $(\overline{T}_{eq})$ in the triplet state at steady-state equilibrium and the triplet relaxation time (τ_T) can be determined by fitting the AC curves to the normalized theoretical AC function [8]. Therefore, it is possible to measure the kinetic parameters such as rates of intersystem crossing, triplet-state depopulation, and the excitation cross section by using tsFCS analysis. Later, Hevekerl *et al.* expanded the electronic state model to a paired donor(D)-acceptor(A) FRET system with a fixed D-A distance (see Fig. S1) [3]. The triplet state population of any fluorophore is sensitive to its excitation rate, independent of whether the fluorophore is excited directly or via FRET (see Fig. S2). Practically, the FRET efficiency (E) is estimated by measuring the fluorescence AC curve of acceptor under a set of donor laser power [3].

In most biological applications of FRET, R may not be unique, especially when the donor and acceptor are linked by a flexible chain. Multiple FRET species manifest a considerable distortion of the triplet-state AC curves of acceptor, and the distribution of acceptor triplet-state relaxation time can be recovered from the distorted triplet-state AC curve of acceptor by using maximum entropy method (MEM) [9], [10]. MEM algorithm [11] has been used to obtain a distribution of diffusion coefficients that fit to fluorescence recovery after photo-bleaching data [12] or fit to diffusional FCS data [9]. Finally, we can calculate the distribution of FRET rate according to an implicit function which maps τ_T of acceptor to k_{FRET} [3], or directly calculate the R distribution.

Although FCS has been widely used to explain the dynamics of basic biophysical processes both in solution and in the living cell, its application for determining the R distribution has not been fully established. We here introduce a MEM-based acceptor tsFCS analysis approach known as tsFCS-FRET to recover the distribution of D-A distances. As a new methodology in FRET measurement, tsFCS-FRET method has its own advantages. First of all, the problems of excitation crosstalk can be solved by introducing the direct excitation term of acceptor and the spectral bleed-through that fluorescence of donor leaking into acceptor channel can be minimized by the suppression algorithm [3]. Furthermore, if the quenching rate ($< 0.1\ \mu s^{-1}$ or $> 10\ \mu s^{-1}$) is out of the triplet state depopulation rate $(\sim 1\ \mu s^{-1})$, the auto-correlation analysis can filter the influence of quenching into the faster region (rotation) or slower region (diffusion) of the AC curve. Even though the quenching reaction has a competitive value of rate with the triplet state depopulation rate, theoretical FCS model of photobleaching or quenching has been well established in the early date [13]. In addition, FCS provides the highest sensitivity for detecting local concentrations of small assemblies in dilute solutions among available analytical techniques. Thus one can easily introduce a parameter of A-to-D concentration ratio factor into the R distribution calculation.

2. Theory and Methodology

2.1. Model of Triplet-State in FCS

The full fluorescence auto-correlation (AC) function can be decomposed as the products of the slow translational diffusion AC function $G_{motion}(\tau)$ and the fast singlet-triplet transitions AC function $G_{triplet}(\tau)$. Focusing on the fast part, the triplet-state AC function reads as [8]

$$G_{triplet}(\tau) = \left[\overline{T}_{eq}/(1-\overline{T}_{eq})\right] \cdot \exp[-\tau/\tau_T] + 1 \tag{1}$$

where $\overline{T}_{eq}$ is the mean fraction of fluorophore within volume element being in their triplet-state at steady-state equilibrium, and τ_T is the triplet relaxation time given by minus reciprocal of eigenvalue λ_3 from the solution of the first-order differential equations (S2) in the supplementary material [8].

Analog to the AC function of a highly heterogeneous system with multiple independent species [14], we here express the triplet-state AC function for a discrete species with different triplet relaxation times $\tau_{T,i}$ as

$$G_{\text{triplet}}(\tau) = \sum_i w_i G_{\text{triplet}}(\tau, \tau_{T,i}) = \sum_i \left[w_i \overline{T}_{\text{eq},i} / (1 - \overline{T}_{\text{eq},i}) \right] \cdot \exp[-\tau/\tau_{T,i}] + \sum_i w_i \tag{2}$$

where w_i are the weights of the components with triplet relaxation time $\tau_{T,i}$.

By defining $f_{\tau_T}(\tau_T)$ as a weight function of a continuous distribution of components with triplet relaxation time τ_T as

$$\int_{\tau_T^L}^{\tau_T^U} f_{\tau_T}(\tau_T) d\tau_T = \sum_i w_i = 1 \tag{3}$$

and modifying (2), $G_{\text{triplet}}(\tau)$ can be rewritten in an integral format

$$G_{\text{triplet}}(\tau) = \int_{\tau_T^L}^{\tau_T^U} A(\tau_T, \overline{T}_{\text{eq}}) \exp[-\tau/\tau_T] d\tau_T + 1 \tag{4}$$

where τ_T^L and τ_T^U are the lower and upper limits for triplet relaxation time appropriate for the sample. The binary function

$$A(\tau_T, \overline{T}_{\text{eq}}) = f_{\tau_T}(\tau_T) \overline{T}_{\text{eq}} / (1 - \overline{T}_{\text{eq}}) \tag{5}$$

denotes the relative amplitude distribution of exponential decay with τ_T in consideration of the fraction population of triplet-state $\overline{T}_{\text{eq}}$.

A simple relation between $\overline{T}_{\text{eq}}$ and τ_T can be obtained by substituting (S5) into (S4) and read as [15]

$$\overline{T}_{\text{eq}} = -k_T \tau_T + 1. \tag{6}$$

Therefore, the binary function $A(\tau_T, \overline{T}_{\text{eq}})$ can be rewritten as

$$A(\tau_T) = f_{\tau_T}(\tau_T)(1/k_T \tau_T - 1) \tag{7}$$

where k_T is constant.

Substituting (7) into (4), the triplet-state AC function can be expressed as the first Fredholm integral equation [16] as follows:

$$G_{\text{triplet}}(\tau) = \int_{\tau_T^L}^{\tau_T^U} A(\tau_T) \exp[-\tau/\tau_T] d\tau_T + 1. \tag{8}$$

The distribution of relative amplitudes $A(\tau_T)$ is obtained by the maximum entropy method [9]. Thus, the weight distribution function of τ_T is determined by

$$f_{\tau_T}(\tau_T) = A(\tau_T) k_T \tau_T / (1 - k_T \tau_T). \tag{9}$$

2.2. Distribution of Distances in Paired Donor-Acceptor System

The A-triplet state parameters $\overline{T}_{\text{eq}}^A$ and τ_T^A determined from the AC curves of the acceptor, are related not only to the intersystem crossing rate k_{ISC}^A and the triplet relaxation rate k_T^A of acceptor but to the energy transfer rate k_{FRET} in (S8) as well [3]. Consequently, we can figure out an

implicit function $k_{\mathrm{FRET}} = \varphi(\tau_{\mathrm{T}}^{A})$, which maps τ_{T}^{A} to k_{FRET}, under a certain donor excitation power according to (S6), (S7), and (S8) [see Fig. S3(a)]. Meanwhile, the energy transfer rate k_{FRET} is a R function [2]

$$k_{\mathrm{FRET}}(R) = \left(1/\tau_0^{D}\right)(R_0/R)^6 \tag{10}$$

where τ_0^{D} is the decay time of donor in the absence of acceptor, R_0 is the Förster radius. Next, we can draw out a monotonic increasing function

$$R = R_0\left[\tau_0^{D}\varphi\left(\tau_T^{A}\right)\right]^{-1/6} \tag{11}$$

which maps τ_{T}^{A} to R [see Fig. S3(c)]. This subsequently leads to the following equality of weight distributions

$$f_R(R)dR = f_{\tau_{\mathrm{T}}^{A}}\left(\tau_{\mathrm{T}}^{A}\right)d\tau_{\mathrm{T}}^{A}. \tag{12}$$

The distribution $f_{\tau_{\mathrm{T}}^{A}}(\tau_{\mathrm{T}}^{A})$ under a certain laser power of donor can be obtained from MEM analysis. Using the numerical calculation of derivative function $|d\tau_{\mathrm{T}}^{A}/dR|$ (see Fig. S3(d)), we finally calculate the R distribution by

$$f_R(R) = f_{\tau_{\mathrm{T}}^{A}}\left(\tau_{\mathrm{T}}^{A}\right)\left|d\tau_{\mathrm{T}}^{A}/dR\right|. \tag{13}$$

2.3. Energy Transfer in Ensembles of Donors and Acceptors

It is easy to introduce an empirical A-to-D concentration ratio factor $x = [\mathrm{A}]/[\mathrm{D}]$ into the FRET E definition [2] with R_0. So the calibrated energy transfer efficiency in ensembles of donors and acceptors can be modified as

$$E_x = xR_0^6/\left(xR_0^6 + R^6\right) \tag{14}$$

and this empirical formula (14) is well consistent with the experimental observations [17]. Based on all above, the calibrated distance in ensembles of donors and acceptors can be rewritten as

$$R_x = R_0\left[x/\left(\tau_0^{D}\varphi\left(\tau_T^{A}\right)\right)\right]^{1/6} \tag{15}$$

where x is A-to-D concentration ratio, and $\varphi(\tau_T^{A})$ is the implicit function of k_{FRET} versus τ_T^{A}. Hence, the distance distribution in ensembles of donors and acceptors can be calibrated by substituting the (15) for the (11) in calculation of distance distribution by using (13).

2.4. Computational Methods

A series of computer simulations are tested to evaluate our approach. The FCS data is generated by incorporating noise using the functional form

$$G_{\mathrm{sim}}(\tau) = G_{\mathrm{theoretical}}(\tau) + G_{\mathrm{noise}}(\tau) \tag{16}$$

where $G_{\mathrm{theoretical}}(\tau)$ is calculated according to (S1), and $G_{\mathrm{noise}}(\tau)$ is calculated at each τ by generating a random number from a Gaussian distribution with its mean equal to $G_{\mathrm{theoretical}}(\tau)$ and standard deviation (SD) proportional to the modified Koppel error value [9], [18].

Fluorescent molecule ATTO 488 and Alexa Fluor 610 are used as mimic donor and acceptor of FRET systems under donor selected excitation. All simulation parameters are chosen based on actual experimental conditions [3]. For motion AC function $G_{\mathrm{motion}}(\tau)$, the particle number is set as $N = 1$ for simplicity and the volume element shape factor is set as $k = 4.117$. Particles are regarded as two species with different diffusibility of $\tau_{D1} = 0.091$ ms and $\tau_{D2} = 0.04$ ms, and $b = 0.3$ denotes their relative concentration ratio. While for triplet-state AC function $G_{\mathrm{triplet}}(\tau)$, the

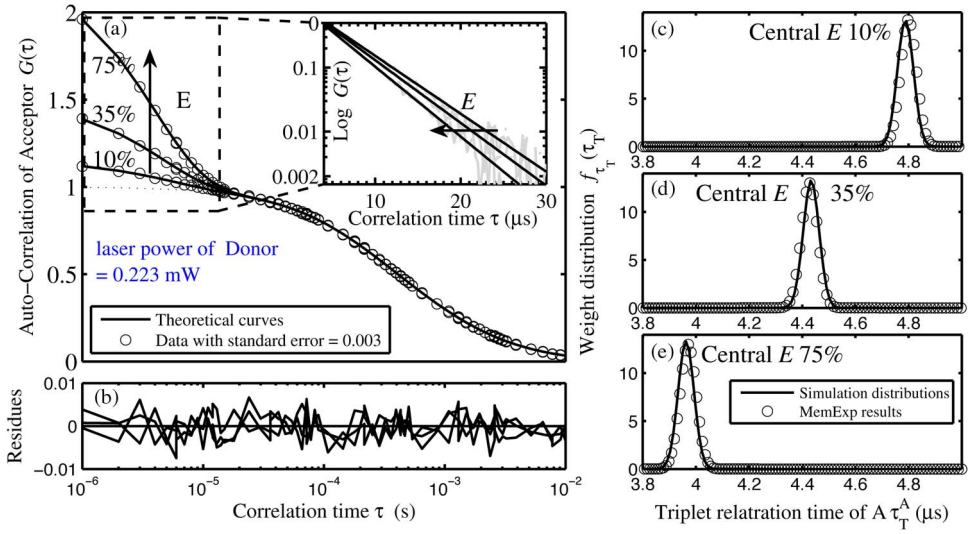

Fig. 1. tsFCS-FRET analyses for FRET *E* system with unimodal distribution. (a) Simulations of triplet-state AC curves of acceptor under 0.2231 mW laser power of the donor. Simulations were performed at a noise level of 0.003, and the central of FRET *E* were set to 10%, 35%, and 75%, respectively. Inset of (a) shows the normalized triplet-state AC curves and the MemExp fitted results in "y-log" scale. (b) Residues of the three simulation data from (a). (c)–(e) Comparing MemExp fitted results (open circles) with pre-assumed distributions of τ_T^A (solid lines) that the central *E* were (c) 10%, (d) 35%, and (e) 75%, respectively.

fluorescent decay rate of donor and acceptor are $k_{rad}^D = 256\ \mu s^{-1}$ and $k_{rad}^A = 255.1\ \mu s^{-1}$, and the triplet state parameters of donor or acceptor are $k_{ISC}^D = 2.2\ \mu s^{-1}$, $k_T^D = 5.1\ \mu s^{-1}$, $k_{ISC}^A = 2.1\ \mu s^{-1}$, and $k_T^A = 0.2\ \mu s^{-1}$, respectively. The laser power of donor is set to 0.223 mW or 2.718 mW at wavelength $\lambda = 488$ nm, and the excitation cross section of donor and acceptor are $\sigma_{exc,488}^D = 2.243 \times 10^{-16}$ cm^2 and $\sigma_{exc,488}^A = 0.079 \times 10^{-16}$ cm^2. Certain FRET *E*, distribution functions $A(\tau)$ or A_i, and the triplet-state relaxation time $\tau_{T,i}^A$ are pre-assumed according to the specific simulations of unimodal distribution, two-species and three-species system. We normalize the triplet-state part of the simulated FCS curves to 0–1 and fit to (8) by MEM algorithm which can be achieved through a free program called MemExp and was further described in supplementary material.

3. Results

We first generated the simulated FCS curves using (16) for three different unimodal distributions of FRET *E* under 0.2231 mW laser power of donor. Simulations were performed at noise level of 0.003 and the central *E* are 10%, 35%, and 75%, respectively. The triplet FCS curves was extracted and normalized to 0–1 [see the inset of Fig. 1(a)]. We fitted the normalized triplet-state AC curves with MemExp and the three fitted results were shown in Fig. 1(c)–(e). We found that the peak coordinates of τ_T^A were always consistent with pre-assumed values, but the height and the width of the fitted distributions may appear occasionally a small deviation from the pre-assumed distributions.

We next produced an acceptor AC curve at noise level of 0.0001. The triplet-state region consist of an exponential function with two equal weights of triplet relaxation time at 4.243 μs and 4.8 μs (correspond to *E* of 50% and 9%). The laser power of donor and the parameters of the motion part were set as the same as the unimodal distribution simulations. We fitted the normalized triplet-state AC curves with MemExp and then analyzed the results by the bimodal Gaussian distribution fitting. The peak coordinates of τ_T^A were consistent with pre-inputted discrete values

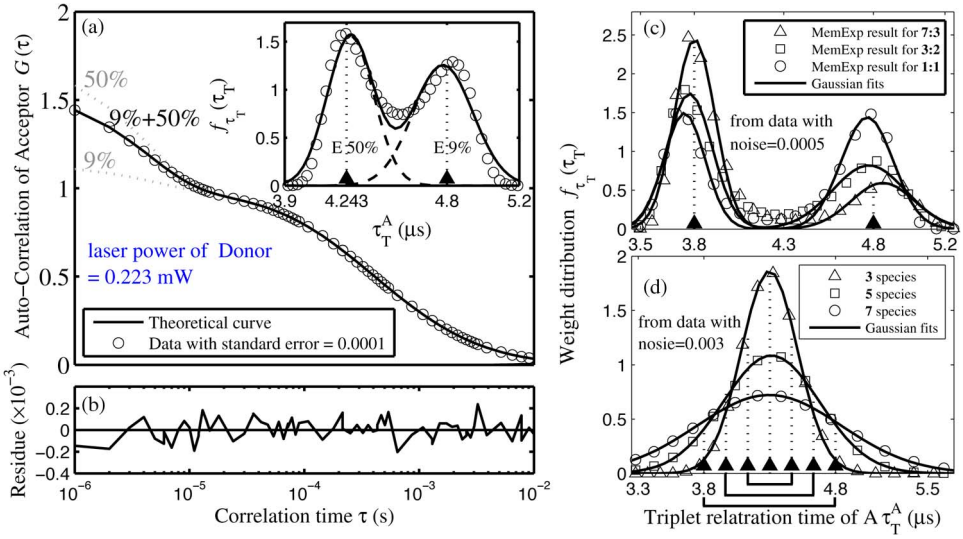

Fig. 2. tsFCS-FRET analyses for FRET *E* system with multiple species. (a) Simulated FCS curve of acceptor under 0.2231 mW laser power of donor with two equal weights FRET *E* of 9% and 50%. Inset of (a) shows the distribution of τ_T^A obtained by MemExp fitting from the simulated data at noise level of 0.0001 (open circles), and the result was fitted to the bimodal Gaussian distribution (solid line). Dash lines denote each peak of Gaussian fitting. (b) Residues of the simulated data from (a). (c) MemExp fittings of two-τ_T^A-species system with unequal weight ratio at noise level of 0.0005. The results of MemExp fittings for systems with different weight ratio of 7 : 3, 3 : 2, and 1 : 1 were indicated by triangles, squares, and circles, respectively. (d) MemExp fittings of multiple-τ_T^A-species system with highly similarity and equal weight at noise level of 0.003. The MemExp fitting results of three species, five species, and seven species were indicated by triangles, squares, and circles, respectively. Solid lines in (c) and (d) were the results from bimodal Gaussian fittings. Black triangles in (a), (c), and (d) indicated the pre-inputted values of τ_T^A.

which were indicated by black triangle in the inset of Fig. 2(a). Although the heights of two peaks were not identical, the areas of two peaks were nearly equal (data not shown). Further, we showed the MemExp fittings of two *E* species system with unequal weights at noise level of 0.0005 in Fig. 2(c). The pre-inputted triplet relaxation time were set to $\tau_{T1} = 3.8\ \mu$s, $\tau_{T2} = 4.8\ \mu$s and the relative amplitudes were set to $A_1 = 0.7$ and $A_2 = 0.3$ (triangles), $A_1 = 0.6$ and $A_2 = 0.4$ (squares), and $A_1 = A_2 = 0.5$ (circles), respectively. From the bimodal Gaussian fitting results, we can see that the peak coordinates as well as the ratios of the peak area were consistent with the pre-input values (data not shown). Lastly, we showed the MemExp fittings of multiple-*E*-species system with highly similarity and equal weight at noise level of 0.003 in Fig. 2(d). The pre-inputted parameters were set to $\tau_{T3,4,5} = [4.13, 4.3, 4.47]\ \mu$s and $A_{3,4,5} = 0.33$ for 3 species (triangles), $\tau_{T2,3,4,5,6} = [3.97, 4.13, 4.3, 4.47, 4.63]\ \mu$s and $A_{2,3,4,5,6} = 0.2$ for 5 species (squares), $\tau_{T1,2,3,4,5,6,7} = [3.8, 3.97, 4.13, 4.3, 4.47, 4.63, 4.8]\ \mu$s and $A_{1,2,3,4,5,6,7} = 0.1429$ for 7 species (circles). The Gaussian distribution fittings showed that the height and the width of distribution were good indicators of the multiple-*E*-species system with highly similarity.

Finally, we tested the method to a three-*E*-species system under different laser power of donor. For laser power 0.223 mW simulation, we set the triplet-state AC curves of acceptor as an exponential function with equal weight of three discrete τ_T^A at 3.86 μs, 4.244 μs, and 4.64 μs, which reflect the *E* of 85%, 50%, and 20%, respectively. The MemExp fitting results for simulated data at noise all level of 0.003, 0.0005, and 0.0001 did not reflect actual pre-inputted values very well [see Fig. 3(a)]. But for laser power 2.718 mW simulation, we set the values of τ_T^A at 1.39 μs, 1.978 μs, and 2.976 μs, which reflect the *E* as the same as previous setting. The MemExp fitting results yielded distributions with three peaks which were close to the actual pre-inputted values in general [see Fig. 3(b)]. At the end, we calculated the *R* distributions from distributions of τ_T^A with assumption that the Föster radius equals 56 angstrom [see Fig. 3 (c) and (d)].

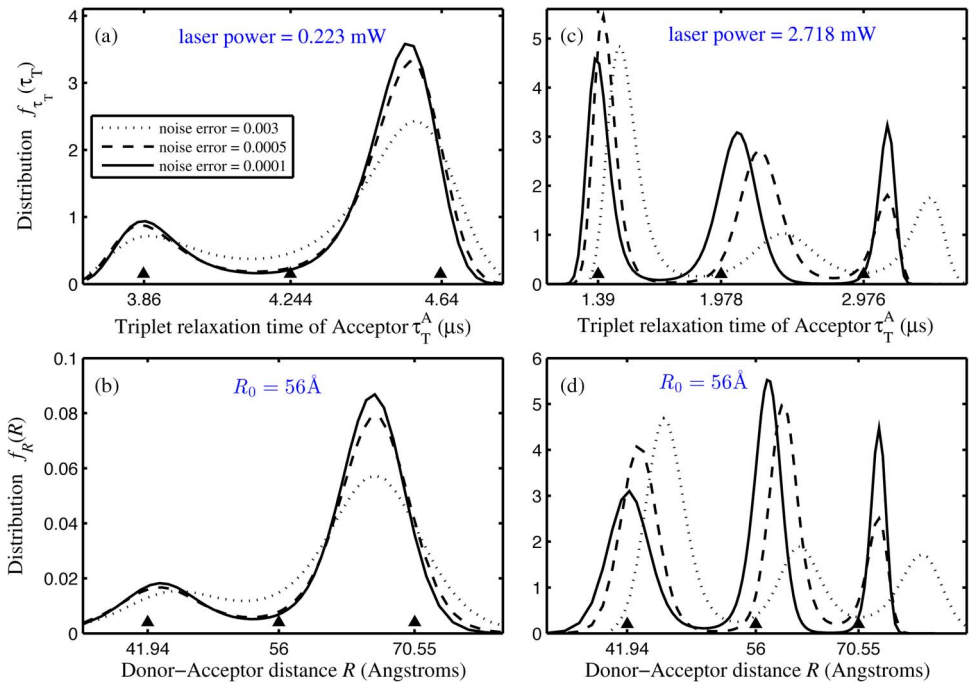

Fig. 3. R distributions of system with three-E-species were calculated from distributions of τ_T^A obtained by tsFCS-FRET analyses. Distributions of τ_T^A under different laser power of donor at (a) 0.223 mW and (c) 2.718 mW were obtained by MemExp fittings of simulated data at noise levels of 0.003, 0.0005, and 0.0001, respectively. R distributions were calculated from the results of MemExp fittings according to (13) for a different laser power of donor at (b) 0.223 mW and (d) 2. 718 mW, respectively.

4. Discussion

Accurate FRET quantification is vital for the determination of intermolecular distances on nano-scale and the scientific communication of FRET index specially for living cell FRET measurement. Our studies suggest that the distribution of D-A distances can be determined by tsFCS-FRET analysis. We performed a series of simulations with different pre-assumed distributions at different noise levels to verify our approach. The verifications were carried out for simulations of the unimodal distribution system, two species system and three species system, respectively. tsFCS-FRET analyses for both unimodal distribution system and two species system (see Figs. 1 and 2) yield a consistent distribution with the actual pre-input. Although tsFCS-FRET analysis for three species system is unsatisfactory at donor low laser power [see Fig. 3(a) and (b)], this analysis yields distributions with three peaks close to the pre-inputted values at higher laser power [see Fig. 3(c) and (d)].

Originally, the common method to evaluate the distribution of D-A distances is based on fluorescence lifetime measurements of the donor. In the case of fluorophores linked by a flexible chain, the analytical distances distribution function is generally assumed to be Gaussian [19]. The R distribution thus can be estimated in generally according to the mean with a standard deviation of the Gaussian distribution [20]. As the fluorescent kinetics of a multiple-FRET-species system is usually very complicated, the assumed R Gaussian distribution is no longer applicable for such highly discrete FRET system. In contrast to the lifetime measurements, our approach is based on the tsFCS analysis of acceptor. It is easy to introduce a continuous τ_T^A distribution of triplet-state in (8). The weight at each point of τ_T^A is set as free variable when fitting the theoretical model to the data via nonlinear least squares (NLS) method. As there is more than one distribution for fitting the data under the constraint of minimizing the deviation chi-square (χ^2), it is necessary to seek another confining condition to ensure an optimal fitting. The second confining

condition is maximizing the value of Shannon entropy stemmed from information theory. Combining the two constraints of minimizing χ^2 and maximizing entropy in NLS fitting generates the MEM algorithm which is further described in supplementary material. By using the MEM recovering technique, our approach can provide numerical solutions not only for unimodal Gaussian distribution [see Figs. 1 and 2(d)] but for distributions with more than one peak as well [see Figs. 2(a), (c), and 3]. Meanwhile, when considering energy transfer from ensemble of donors to multiple acceptors, the modified fluorescence decay formula contains a parameter of acceptors concentration [A] which must be predetermined by other fluorescent technique. In our approach, concentrations of both donors [D] and acceptors [A] can be easily measured, because FCS provides the highest sensitivity for detecting local concentrations of small assemblies in dilute solutions. Therefore, it is more easily to introduce an empirical A-to-D concentration ratio factor x for calculation of the spectral overlap integral item to calibrate the distance distributions for FRET system with multiple acceptors.

The reasonability of introducing the empirical factor x for the modified FRET E calculation in (14) is that the probability of energy transfer in ensembles of donors to acceptors is different from the paired D-A molecule. Generally, the definition of Förster radius R_0 leads to calculation of the spectral overlap integral term J [2], and the J is always normalized by the whole integrated intensity of fluorescence of donor to emphasize the energy transfer rate in paired D-A molecule. The normalized fluorescence spectrum of donor is characteristic of a given donor fluorophore and reflects the distribution of the probability of the various transitions from the lowest vibrational level of the first excited state S_1 to the various vibrational levels of the ground state S_0 [21]. From this basic point, the spectral overlap integral item J_x in ensembles of donors to acceptors can be regarded as the it's normalized by $1/x$ unit of intensity of donor per one unit of absorption of acceptor.

One important issue related to the correct usage of FRET in calculating distance distributions between fluorophores is the predetermination of the orientation factor κ^2 $(0 < \kappa^2 < 4)$ [22]. Because the Föster radius was defined as a function of the orientation factor [2], uncertainties in the orientation factor will undermine the quality of information that can be retrieved from a FRET experiment. If the fluorophores are assumed to be spheres with rapid rotational diffusion through all possible orientations over the time span of energy transfer, a dynamic average value of orientation factor $(\langle\kappa^2\rangle = 2/3)$ can be used for computation of R_0 and D-A distance distribution [23], [24]. However, this can lead to significant error in unfavorable cases especially uncertainty is still widely regarded as an inconvenience of hindered rotations in membrane [22]. Practically, the value of κ^2 can be estimated by experimental techniques from polarization anisotropy measurements [25] or theoretical techniques from molecular dynamics simulations [26]. More detail about quantitative analysis of κ^2 is discussed in the extend Förster theory (EFT) which makes use of Brownian dynamics simulation [27], [28]. Determining orientation would assist to understanding the changes in the rotational freedom of molecular samples. In addition, knowledge about rotational freedom of fluorophores can work backward to the value of κ^2. Furthermore, FCS models can be used for measuring rotational diffusion even at the very beginning of FCS [29], [30], and this option refocus attention on resolving membrane biophysics recently. In our approach, it's possible to investigate the relative rotational mobility between dipoles of donor and acceptor fluorophores by using of acceptor FCS analysis. In fact, our approach implies an experimental determination of the orientation factor κ^2 in FRET measurements without assistance from the other technique.

In consideration of the inevitably non-uniform excitation intensity in the detection volume, we provide a preliminary discussion, in the supplementary material, on how Gaussian profile laser excitation influences the distribution of triplet state in FRET-mediated tsFCS measurement.

5. Conclusion

In summary, this paper, for the first time, developed a triplet-state FCS analysis-based FRET simulation method (tsFCS-FRET) to resolve the donor-acceptor distance distribution of a system

with multiple FRET species. Theoretically, we make efforts to solve three major difficulties in FRET measurements: spectral cross-talks, fluorescence quenching, and multiple acceptors. Simulations for one-species to three-species systems showed that tsFCS-FRET may be used to resolve the *R* and *E* distributions of a FRET system containing multiple *E* species. The method also implies a potential to measure the orientation factor κ^2, and we will launch this theorem research in the near future. The accuracy of this method depends on the data noise level and the employed analysis algorithm.

References

[1] T. Förster, "Zwischenmolekulare energiewanderung und fluoreszenz," *Ann. Phys.*, vol. 437, no. 1/2, pp. 55–75, 1948.
[2] J. R. Lakowicz, *Energy Transfer*, 3rd ed. New York, NY, USA: Springer-Verlag, Sep. 2006, ch. 13, pp. 443–475.
[3] H. Hevekerl, T. Spielmann, A. Chmyrov, and J. Widengren, "Förster resonance energy transfer beyond 10 nm: Exploiting the triplet state kinetics of organic fluorophores," *J. Phys. Chem., B.*, vol. 115, no. 45, pp. 13 360–13 370, 2011.
[4] T. C. Voss, I. A. Demarco, and R. N. Day, "Quantitative imaging of protein interactions in the cell nucleus," *Biotechniques*, vol. 38, no. 3, pp. 413–424, 2005.
[5] J. Zhang, R. E. Campbell, A. Y. Ting, and R. Y. Tsien, "Creating new fluorescent probes for cell biology," *Nat. Rev. Mol. Cell Biol.*, vol. 3, no. 12, pp. 906–918, Dec. 2002.
[6] P. Schwille, "Fluorescence correlation spectroscopy and its potential for intracellular applications," *Cell Biochem. Biophys.*, vol. 34, no. 3, pp. 383–408, 2001.
[7] R. Rigler, U. Mets, J. Widengren, and P. Kask, "Fluorescence correlation spectroscopy with high count rate and low background: Analysis of translational diffusion," *Eur. Biophys. J.*, vol. 22, no. 3, pp. 169–175, Aug. 1993.
[8] J. Widengren, U. Mets, and R. Rigler, "Fluorescence correlation spectroscopy of triplet states in solution: A theoretical and experimental study," *J. Phys. Chem.*, vol. 99, no. 36, pp. 13 368–13 379, 1995.
[9] P. Sengupta, K. Garai, J. Balaji, N. Periasamy, and S. Maiti, "Measuring size distribution in highly heterogeneous systems with fluorescence correlation spectroscopy," *Biophys. J.*, vol. 84, no. 3, pp. 1977–1984, 2003.
[10] P. J. Steinbach, R. Ionescu, and C. R. Matthews, "Analysis of kinetics using a hybrid maximum-entropy/nonlinear-least-squares method: Application to protein folding," *Biophys. J.*, vol. 82, no. 4, pp. 2244–2255, 2002.
[11] J. Skilling and R. K. Bryan, "Maximum entropy image reconstruction - general algorithm," *Monthly Notices R. Astron. Soc.*, vol. 211, no. 1, pp. 111–124, 1984.
[12] N. Periasamy and A. S. Verkman, "Analysis of fluorophore diffusion by continuous distributions of diffusion coefficients: Application to photobleaching measurements of multicomponent and anomalous diffusion," *Biophys. J.*, vol. 75, no. 1, pp. 557–567, 1998.
[13] J. Widengren and R. Rigler, "Mechanisms of photobleaching investigated by fluorescence correlation spectroscopy," *Bioimaging*, vol. 4, pp. 149–157, 1996.
[14] J. M. Paredes *et al.*, "Early amyloidogenic oligomerization studied through fluorescence lifetime correlation spectroscopy," *Int. J. Mol. Sci.*, vol. 13, no. 8, pp. 9400–9418, 2012.
[15] J. Strömqvist *et al.*, "Quenching of triplet state fluorophores for studying diffusion-mediated reactions in lipid membranes," *Biophys. J.*, vol. 99, no. 11, pp. 3821–3830, 2010.
[16] S. N. Baginskaya and E. G. Davydov, "Fredholm equations of the first kind," *Comput. Math. Mod.*, vol. 8, pp. 226–230, 1997.
[17] I. L. Medintz *et al.*, "Self-assembled nanoscale biosensors based on quantum dot fret donors," *Nat. Mater.*, vol. 2, no. 9, pp. 630–638, 2003.
[18] D. E. Koppel, "Statistical accuracy in fluorescence correlation spectroscopy," *Phys. Rev., A.*, vol. 10, no. 6, pp. 1938–1945, Dec. 1974.
[19] B. Valeur, *Resonance Energy Transfer and its Applications*. Hoboken, NJ, USA: Wiley-VCH Verlag GmbH, 2001, ch. 9, pp. 247–271.
[20] S. Batabyal, T. Mondol, and S. K. Pal, "Picosecond-resolved solvent reorganization and energy transfer in biological and model cavities," *Biochimie*, vol. 95, no. 6, pp. 1127–1135, Jun. 2013.
[21] B. Valeur, *Characteristics of Fluorescence Emission*. Hoboken, NJ, USA: Wiley-VCH Verlag GmbH, 2001, ch. 3, pp. 34–70.
[22] L. M. S. Loura, "Simple estimation of Förster resonance energy transfer (FRET) orientation factor distribution in membranes," *Int. J. Mol. Sci.*, vol. 13, no. 11, pp. 15 252–15 270, 2012.
[23] B. Van Der Meer, G. Coker, and S. Chen, *Resonance Energy Transfer: Theory and Data*. Hoboken, NJ, USA: Wiley, 1994.
[24] C. G. dos Remedios and P. D. Moens, "Fluorescence resonance energy transfer spectroscopy is a reliable 'ruler' for measuring structural changes in proteins. Dispelling the problem of the unknown orientation factor," *J. Struct. Biol.*, vol. 115, no. 2, pp. 175–185, 1995.
[25] B. Saccá, S. Fiori, and L. Moroder, "Studies of the local conformational properties of the cell-adhesion domain of collagen type IV in synthetic heterotrimeric peptides," *Biochem.*, vol. 42, no. 12, pp. 3429–3436, 2003.
[26] L. M. S. Loura and J. P. P. Ramalho, "Recent developments in molecular dynamics simulations of fluorescent membrane probes," *Molecules*, vol. 16, no. 7, pp. 5437–5452, 2011.
[27] P. Håkansson, M. Isaksson, P.-O. Westlund, and L. B.-Å. Johansson, "Extended Förster theory for determining intra-protein distances. 1. The κ^2-dynamics and fluorophore reorientation," *J. Phys. Chem., B.*, vol. 108, no. 44, pp. 17 243–17 250, 2004.

[28] M. Isaksson, N. Norlin, P.-O. Westlund, and L. B.-Å. Johansson, "On the quantitative molecular analysis of electronic energy transfer within donor-acceptor pairs," *Phys. Chem. Chem. Phys.*, vol. 9, pp. 1941–1951, 2007.
[29] M. Ehrenberg and R. Rigler, "Rotational Brownian motion and fluorescence intensity fluctuations," *Chem. Phys.*, vol. 4, no. 3, pp. 390–401, 1974.
[30] C. M. Pieper and J. Enderlein, "Fluorescence correlation spectroscopy as a tool for measuring the rotational diffusion of macromolecules," *Chem. Phys. Lett.*, vol. 516, pp. 1–11, 2011.